© 2014. Published by The Company of Biologists Ltd | Development (2014) 141, 4751-4762 doi:10.1242/dev.117200

RESEARCH ARTICLE

Epithelial β1 integrin is required for lung branching morphogenesis and alveolarization

Erin J. Plosa[1], Lisa R. Young[2,3,4], Peter M. Gulleman[2], Vasiliy V. Polosukhin[3], Rinat Zaynagetdinov[3], John T. Benjamin[1], Amanda M. Im[1], Riet van der Meer[1], Linda A. Gleaves[3], Nada Bulus[5], Wei Han[3], Lawrence S. Prince[6], Timothy S. Blackwell[3,4,7,8] and Roy Zent[4,5,7,8,*]

ABSTRACT

Integrin-dependent interactions between cells and extracellular matrix regulate lung development; however, specific roles for β1-containing integrins in individual cell types, including epithelial cells, remain incompletely understood. In this study, the functional importance of β1 integrin in lung epithelium during mouse lung development was investigated by deleting the integrin from E10.5 onwards using surfactant protein C promoter-driven Cre. These mutant mice appeared normal at birth but failed to gain weight appropriately and died by 4 months of age with severe hypoxemia. Defects in airway branching morphogenesis in association with impaired epithelial cell adhesion and migration, as well as alveolarization defects and persistent macrophage-mediated inflammation were identified. Using an inducible system to delete β1 integrin after completion of airway branching, we showed that alveolarization defects, characterized by disrupted secondary septation, abnormal alveolar epithelial cell differentiation, excessive collagen I and elastin deposition, and hypercellularity of the mesenchyme occurred independently of airway branching defects. By depleting macrophages using liposomal clodronate, we found that alveolarization defects were secondary to persistent alveolar inflammation. β1 integrin-deficient alveolar epithelial cells produced excessive monocyte chemoattractant protein 1 and reactive oxygen species, suggesting a direct role for β1 integrin in regulating alveolar homeostasis. Taken together, these studies define distinct functions of epithelial β1 integrin during both early and late lung development that affect airway branching morphogenesis, epithelial cell differentiation, alveolar septation and regulation of alveolar homeostasis.

KEY WORDS: Extracellular matrix, Branching morphogenesis, Alveolar epithelial cell, Differentiation, Inflammation, Reactive oxygen species

INTRODUCTION

Embryonic lung development occurs as a result of epithelial-mesenchymal interactions that are initiated when the bronchial buds grow into the surrounding mesoderm. The buds undergo iterative branching morphogenesis to give rise to the respiratory tree, terminal saccules and alveoli, whereas the mesoderm forms the lung fibroblasts and the pulmonary vasculature (Cardoso and Lu, 2006; Hogan, 1999). This complex pattern of development depends on a variety of factors, including expression of mesenchymal-derived signaling molecules and their receptors on epithelium, as well as cell-extracellular matrix (ECM) interactions (McGowan, 1992; Morrisey and Hogan, 2010).

The lung basement membrane (BM) is composed primarily of collagen IV, laminins, nidogen and proteoglycans (Thibeault et al., 2003; Wasowicz et al., 1998), and several previous studies have shown that distinct laminin chains are required for normal lung branching morphogenesis, lobar septation and alveolarization (Nguyen et al., 2005, 2002; Nguyen and Senior, 2006; Willem et al., 2002). The major integrins that affect cell-ECM interactions during lung development are the laminin receptors α3β1, α6β1 and α6β4 (De Arcangelis et al., 1999; Georges-Labouesse et al., 1996; Has et al., 2012; Kim et al., 2009; Kreidberg et al., 1996; Nicolaou et al., 2012). Of the laminin receptors, integrin α3β1 has been most extensively investigated. Lungs from constitutive integrin α3-null mice fail to branch into bronchioles (Kreidberg et al., 1996), and mice null for both integrin α3 and α6 have severe lung hypoplasia (De Arcangelis et al., 1999). Surprisingly, mice with a lung epithelial-specific deletion of α3 integrin have a normal lifespan with normal airway branching but subtle defects in epithelial differentiation (Kim et al., 2009). Recently, lung hypoplasia due to integrin α3 mutations has been identified as a cause of early childhood mortality (Has et al., 2012; Nicolaou et al., 2012). The RGD-binding integrin α8β1 has also been shown to regulate lung development as constitutive integrin α8-null mice have abnormally fused medial and caudal lobes of the lung, as well as subtle abnormalities in airway division (Benjamin et al., 2009).

β1 integrin is the major isoform of the eight β-integrin subunits, and is the β-integrin subunit present in 12 of the 24 known α-β integrin heterodimers (Pozzi and Zent, 2011). When β1 integrin is selectively deleted in lung epithelium at the time of endodermal tracheal outgrowth (E9.5) using a Shh promoter-driven Cre, mice develop a severe branching morphogenesis defect that blocks development at the level of primary bronchi, making it impossible to determine the role of β1 integrin at later stages of development (Chen and Krasnow, 2012). To elucidate possible crucial functions of β1 integrin beyond the initial stages of lung development, we generated mice with an epithelial-targeted deletion of β1 integrin using a surfactant protein C (SP-C; also known as SFTPC) promoter-driven Cre, which is expressed in the lung epithelium at E10.5 (Okubo et al., 2005). Analysis of these mice showed that β1 integrin regulates a variety of crucial epithelial cell processes required for normal lung development and homeostasis.

[1]Department of Pediatrics, Division of Neonatology, Vanderbilt University Medical Center, Nashville, TN 37232, USA. [2]Department of Pediatrics, Division of Pulmonary Medicine, Vanderbilt University Medical Center, Nashville, TN 37232, USA. [3]Department of Medicine, Division of Allergy, Pulmonary, and Critical Care Medicine, Vanderbilt University Medical Center, Nashville, TN 37232, USA. [4]Department of Cell and Developmental Biology, Vanderbilt University Medical Center, Nashville, TN 37232, USA. [5]Department of Medicine, Division of Nephrology, Vanderbilt University Medical Center, Nashville, TN 37232, USA. [6]Department of Pediatrics, Division of Neonatology, University of California San Diego, San Diego, CA 92103, USA. [7]Department of Cancer Biology, Vanderbilt University Medical Center, Nashville, TN 37232, USA. [8]Nashville Veterans Affairs Medical Center, Nashville, TN 37232, USA.

*Author for correspondence (roy.zent@vanderbilt.edu)

Received 30 August 2014; Accepted 9 October 2014

Development (2014) 141, 4751-4762 doi:10.1242/dev.117200

RESULTS

Epithelial-specific β1 integrin deficiency results in abnormal lung structure and reduced lifespan

We deleted β1 integrin in the lung epithelium from E10.5 onwards by crossing SP-C-Cre mice with integrin $\beta1^{f/f}$ ($\beta1^{f/f}$) mice (hereafter called $\beta1^{SP\text{-}C.Cre}$ mice). By E13, β1 integrin was selectively deleted in the proximal and distal lung epithelium as shown by immunostaining of embryonic airways (Fig. 1A,B). $\beta1^{SP\text{-}C.Cre}$ mice were born in the normal Mendelian ratio; however, few survived longer than 4 months (Fig. 1C). $\beta1^{SP\text{-}C.Cre}$ mice grew poorly and were significantly smaller than age-matched littermate control $\beta1^{f/f}$ (Fig. 1D) and heterozygote SP-C-Cre; $\beta1^{f/WT}$ mice (data not shown). Interestingly, $\beta1^{SP\text{-}C.Cre}$ mice had normal oxygen saturation at birth, but by 8 weeks they were severely hypoxemic with a mean oxygen saturation of 79% (Fig. 1E). Thus, deleting β1 integrin in the lung epithelium results in a lethal phenotype with severe hypoxia.

Despite having lower body weight, adult $\beta1^{SP\text{-}C.Cre}$ mouse lungs were larger and weighed more (35.8±3 mg versus 24.2±2 mg) than littermate $\beta1^{f/f}$ mice (Fig. 2A,B). Histological examination of lung parenchyma from P28 and older $\beta1^{SP\text{-}C.Cre}$ mice revealed dilated airspaces surrounded by thickened, hypercellular alveolar septa with type II epithelial cell hyperplasia and increased numbers of macrophages (Fig. 2C-K). $\beta1^{SP\text{-}C.Cre}$ lungs showed sustained airspace enlargement at 3 months of age (Fig. 2H-K). Alveolar size, as measured by calculating the mean linear intercept, in P28 $\beta1^{SP\text{-}C.Cre}$ mice was approximately double the value in controls (Fig. 2G). Heterozygotes were indistinguishable from littermate control $\beta1^{SP\text{-}C.Cre}$ mice in histological examinations at both time points (data not shown). Thus deleting β1 integrin from the lung epithelium results in large and dilated airspaces, thickened inter-alveolar septa, abnormal epithelial cell differentiation and influx of alveolar macrophages, probably explaining the hypoxemia and premature mortality observed in these mice.

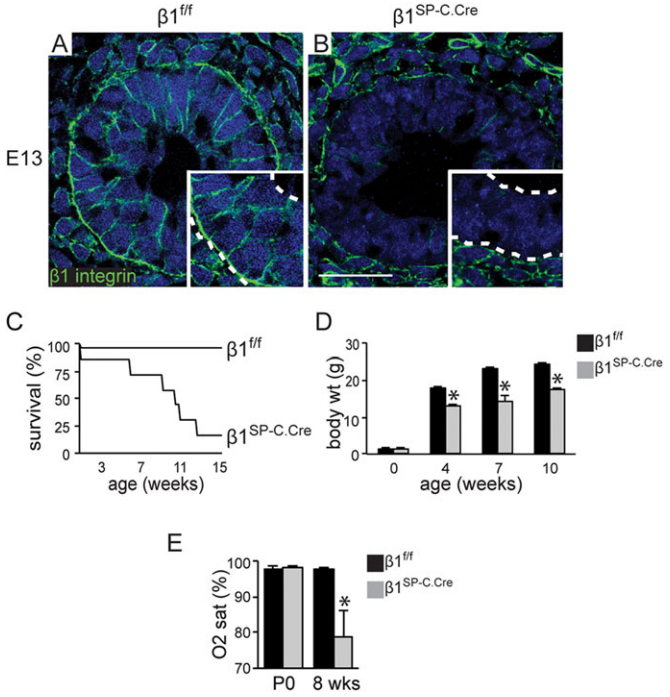

Fig. 1. β1 integrin is specifically deleted in the lung epithelium. (A,B) β1 integrin immunostaining showing lung epithelial-specific deletion in E13 $\beta1^{SP\text{-}C.Cre}$ mice (dashed lines outline the epithelium). (C) Kaplan–Meier survival curve for $\beta1^{SP\text{-}C.Cre}$ and $\beta1^{f/f}$ mice (n=7 mice in each group). (D) Growth chart for $\beta1^{SP\text{-}C.Cre}$ and $\beta1^{f/f}$ mice (for $\beta1^{SP\text{-}C.Cre}$ mice, n=5 at P0 and 4 weeks, n=4 at 7 weeks, and n=3 at 10 weeks as survival declined; n=14 for $\beta1^{f/f}$ mice at all time points). (E) Oxygen saturations in $\beta1^{SP\text{-}C.Cre}$ and $\beta1^{f/f}$ mice [for newborn pups (P0): n=4 $\beta1^{SP\text{-}C.Cre}$ mice, n=9 $\beta1^{f/f}$ mice; for 8-week-old mice: n=6 $\beta1^{SP\text{-}C.Cre}$ mice, n=4 $\beta1^{f/f}$ mice]. *P<0.05 between $\beta1^{SP\text{-}C.Cre}$ and $\beta1^{f/f}$ mice. Scale bar: in B, 25 µm for A,B.

Deleting β1 integrin in lung epithelium results in a branching morphogenesis defect

Analysis of the airways in adult $\beta1^{SP\text{-}C.Cre}$ mice revealed a paucity of terminal bronchioles, indicative of a branching morphogenesis defect. We therefore examined lung histology near the initiation, mid-point and completion of branching morphogenesis. Although no branching defect was identified at E13 during early branching morphogenesis (Fig. 3A,B), abnormal branching was seen at E15. At E15, $\beta1^{SP\text{-}C.Cre}$ airways were similar in size to controls but fewer in number and separated by a thickened interstitium (Fig. 3C,D). This branching defect was even more evident by E18, where there was a marked reduction of airways in $\beta1^{SP\text{-}C.Cre}$ mice (Fig. 3E,F) as verified by quantification of histological sections (147±14 airways per mm^2 in $\beta1^{SP\text{-}C.Cre}$ lungs compared with 259±13 airways per mm^2 in $\beta1^{f/f}$ mice; mean±s.e.m.) (Fig. 3I). In contrast to the proximal to distal airway narrowing seen in normal mice, there were a number of large airways found in the peripheral lung of the $\beta1^{SP\text{-}C.Cre}$ mice (Fig. 3F, asterisks). Consistent with observations indicating fewer airways in $\beta1^{SP\text{-}C.Cre}$ mice, the airspace volume density of E18 $\beta1^{SP\text{-}C.Cre}$ lungs was significantly less (29±1%) than $\beta1^{f/f}$ lungs (46±1%) (Fig. 3J). Airspaces in lungs of $\beta1^{SP\text{-}C.Cre}$ mice at P0 were fewer in number and larger in histological examinations (Fig. 3G,H).

In addition to abnormal airway branching at E18 in $\beta1^{SP\text{-}C.Cre}$ mice, hypercellularity of the interstitium was evident. By Ki67 (also known as MKI67) staining, we identified increased cellular proliferation in the interstitium of E18 $\beta1^{SP\text{-}C.Cre}$ lungs compared with $\beta1^{f/f}$ lungs (29±2% versus 7±1% Ki67-positive cells) (Fig. 3K-M). The proliferating cell population was primarily non-epithelial in $\beta1^{SP\text{-}C.Cre}$ lungs as verified by co-immunostaining for the mitotic marker phosphohistone H3 (PHH3) and the epithelial marker E-cadherin (Fig. 3N-P). A total of 58.7±0.5% and 39.2±0.5% of proliferating (PHH3+) cells were non-epithelial in $\beta1^{SP\text{-}C.Cre}$ and $\beta1^{f/f}$ lungs respectively (P<0.05). By contrast, there was no significant difference in apoptosis between $\beta1^{SP\text{-}C.Cre}$ and $\beta1^{f/f}$ lungs at this time point (supplementary material Fig. S1E). Thus, deleting β1 integrin in the lung epithelium results in a branching morphogenesis defect and increased interstitial cell proliferation.

To better define the mechanism of branching defects in $\beta1^{SP\text{-}C.Cre}$ mice, we examined E15 fetal lung explants. Compared with controls, significantly less new branching occurred in $\beta1^{SP\text{-}C.Cre}$ lung explants cultured for 12 and 48 h (Fig. 4A-E). When the velocity of the leading epithelial edge of peripheral airways was tracked in these cultures using time-lapse microscopy, we measured a decreased outward velocity of the epithelial edge in $\beta1^{SP\text{-}C.Cre}$ explants (3.2±0.05 µm/h versus 2.9±0.06 µm/h in $\beta1^{f/f}$ explants) (Fig. 4F). Although no difference in explant size was identified between $\beta1^{SP\text{-}C.Cre}$ and $\beta1^{f/f}$ lung explants at 48 h (data not shown), the distance from the epithelial basement membrane to the explant edge was greater in $\beta1^{SP\text{-}C.Cre}$ lung explants compared with controls (2.08±0.5 µm versus 0.13±0.6 µm), indicative of decreased outward epithelial growth and/or increased mesenchymal proliferation (Fig. 4G-I). These data suggest that loss of epithelial β1 integrin disrupts epithelial migration, a key cellular process during branching morphogenesis. To further investigate the migratory phenotype of β1 integrin-null lung epithelial cells, we isolated type II epithelial cells from P28 $\beta1^{SP\text{-}C.Cre}$ and $\beta1^{f/f}$ mice and

Development (2014) 141, 4751-4762 doi:10.1242/dev.117200

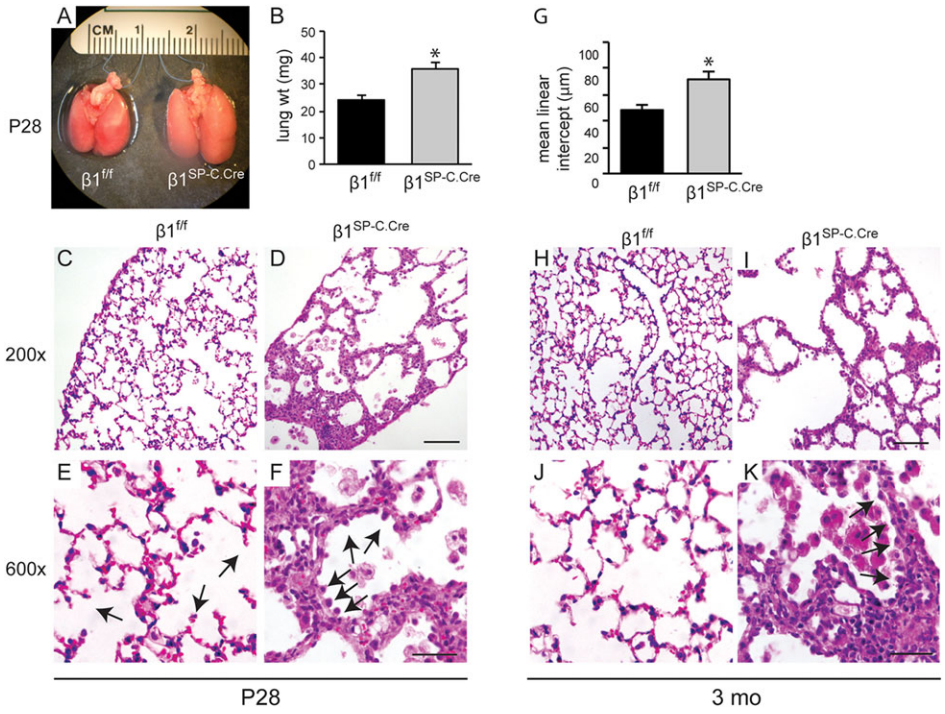

Fig. 2. $\beta1^{SP\text{-}C.Cre}$ mice have dilated airspaces and thickened alveolar septa. (A) Gross appearance of P28 $\beta1^{SP\text{-}C.Cre}$ and $\beta1^{f/f}$ lungs. (B) $\beta1^{SP\text{-}C.Cre}$ mice have increased dry lung weights compared with $\beta1^{f/f}$ mice (n=5 $\beta1^{SP\text{-}C.Cre}$ mice, n=3 $\beta1^{f/f}$ mice). (C,D) Dilated airspaces with thickened alveolar septa seen in H&E-stained paraffin sections of P28 $\beta1^{SP\text{-}C.Cre}$ lungs (labeled 200×). (E,F) Type II cell (arrows) hyperplasia in P28 $\beta1^{SP\text{-}C.Cre}$ lungs (labeled 600×). (G) The mean linear intercept is greater in $\beta1^{SP\text{-}C.Cre}$ versus $\beta1^{f/f}$ mice (n=3 $\beta1^{SP\text{-}C.Cre}$ mice, n=4 $\beta1^{f/f}$ mice, 10 sections per mouse). (H,I) Dilated airspaces and thickened alveolar septa persist throughout the lifespan of $\beta1^{SP\text{-}C.Cre}$ mice (labeled 200×). (J,K) Type II cell (arrows) hyperplasia demonstrated in 3-month-old (3 mo) $\beta1^{SP\text{-}C.Cre}$ mice (labeled 600×). *P<0.05 between $\beta1^{SP\text{-}C.Cre}$ and $\beta1^{f/f}$ mice. Scale bars: in D, 100 μm for C,D; in I, 100 μm for H,I; in F, 25 μm for E,F; in K, 25 μm for J,K.

confirmed β1 integrin deletion by immunoblotting (Fig. 4J). These cells had a marked adhesion defect (74±11% $\beta1^{f/f}$ versus 18±18% $\beta1^{SP\text{-}C.Cre}$ cells adhered) on purified laminin 511, a major laminin isoform found in the fetal lung basement membrane that is required for normal lung development (Nguyen et al., 2005) (Fig. 4K). In addition, these cells had a major haptotactic migration defect on laminin 511 (Fig. 4L). Taken together, these data indicate a role for β1 integrin in alveolar epithelial adhesion and migration, and suggest a potential mechanism for the branching defect seen in $\beta1^{SP\text{-}C.Cre}$ mice.

Lung epithelial-specific deletion of β1 integrin disrupts alveolarization

In addition to an airway branching defect, adult $\beta1^{SP\text{-}C.Cre}$ mice had dilated alveoli with thickened alveolar septa, suggestive of an additional alveolarization defect. We therefore examined $\beta1^{SP\text{-}C.Cre}$ lungs at P7 and P14 to identify defects in secondary septation. Airspace enlargement was seen by P7 (Fig. 5A,B) in $\beta1^{SP\text{-}C.Cre}$ lungs and this was even more obvious at P14 (Fig. 5C,D). In addition, P14 $\beta1^{SP\text{-}C.Cre}$ alveolar septa were hypercellular and thickened suggesting increased ECM deposition. We quantified the differences in alveolar size by measuring the average alveolar diameter in P14 $\beta1^{SP\text{-}C.Cre}$ and $\beta1^{f/f}$ mice (50±2 μm in $\beta1^{SP\text{-}C.Cre}$ lungs versus 30±3.5 μm in $\beta1^{f/f}$ lungs; mean±s.e.m.) (Fig. 5G). To determine whether loss of β1 integrin disrupted secondary septation, we quantified the number of secondary crests and found that $\beta1^{SP\text{-}C.Cre}$ lungs had significantly fewer secondary crests per high-power field than $\beta1^{f/f}$ control littermates (26±2 crests in $\beta1^{SP\text{-}C.Cre}$ lungs versus 92±5 crests in $\beta1^{f/f}$ lungs) (Fig. 5H). Similar to the above studies in embryonic lungs, we found that the hypercellularity noted in the interalveolar spaces during alveolarization was due to increased cell proliferation and not decreased apoptosis, as Ki67 staining was increased in $\beta1^{SP\text{-}C.Cre}$ mice compared with $\beta1^{f/f}$ controls (25±2% versus 10±1%), whereas immunostaining for cleaved caspase 3 was not different between the two genotypes (Fig. 5I,J). When we defined the composition of interstitial ECM at P14, we noted a marked increase in elastin and collagen I, but not collagen IV, in $\beta1^{SP\text{-}C.Cre}$ alveolar septa compared with that amount in alveolar septa from $\beta1^{f/f}$ lungs (Fig. 5K-P). Despite disruptions to the epithelium and ECM, the vasculature developed in close proximity to the alveolar epithelium in $\beta1^{SP\text{-}C.Cre}$ mice because staining for the endothelial marker CD31 demonstrated that there were intact capillary networks adjacent to the alveolar surface in both $\beta1^{f/f}$ and $\beta1^{SP\text{-}C.Cre}$ mice (supplementary material Fig. S1C,D). Taken together, these data suggest that deleting β1 integrin disrupts alveolar septal structure by reducing secondary septation and increasing mesenchymal cell proliferation and ECM deposition.

Loss of epithelial β1 integrin results in abnormal alveolar epithelial cell differentiation

The histological features of $\beta1^{SP\text{-}C.Cre}$ lungs suggested that there were β1 integrin-dependent defects in epithelial cell differentiation. Abundant cuboidal epithelial cells lined the peripheral airways of E18 $\beta1^{SP\text{-}C.Cre}$ lungs (Fig. 6B, arrows), compared with a more differentiated flattened epithelium in control mice (Fig. 6A, arrowheads). After birth, periodic acid schiff staining revealed that there were epithelial cells with a marked increase in glycoprotein deposition in large airways of P14 $\beta1^{SP\text{-}C.Cre}$ mice, which was not present in the $\beta1^{f/f}$ mice (Fig. 6C,D). In addition to airways, we evaluated epithelial structure in lung parenchyma. Alveoli of P14 $\beta1^{SP\text{-}C.Cre}$ mice showed increased Nkx2.1 and pro-SP-C immunostaining consistent with type II cell hyperplasia (Fig. 6E-J). Transmission electron microscopic images of representative type II cells from adult $\beta1^{SP\text{-}C.Cre}$ and $\beta1^{f/f}$ mice demonstrated that type II alveolar epithelial cells lining the thickened septa (Fig. 6L, arrows) in $\beta1^{SP\text{-}C.Cre}$ mice were not only hyperplastic, but also had abnormal cellular morphology (Fig. 6K-M) characterized by fewer lamellar bodies (demarcated by arrowheads), a larger nucleus and diminished cytoplasm. As these cells appeared to have a hybrid phenotype (i.e. between that of a type I and type II cell), we immunostained P14 lungs for the type I marker T1α (also known as PDPN) and the type II cell marker pro-SP-C and found numerous dual-positive $\beta1^{SP\text{-}C.Cre}$ epithelial cells lining the dilated airspaces (Fig. 6N,O), suggesting that β1 integrin regulates alveolar epithelial cell differentiation.

Development (2014) 141, 4751-4762 doi:10.1242/dev.117200

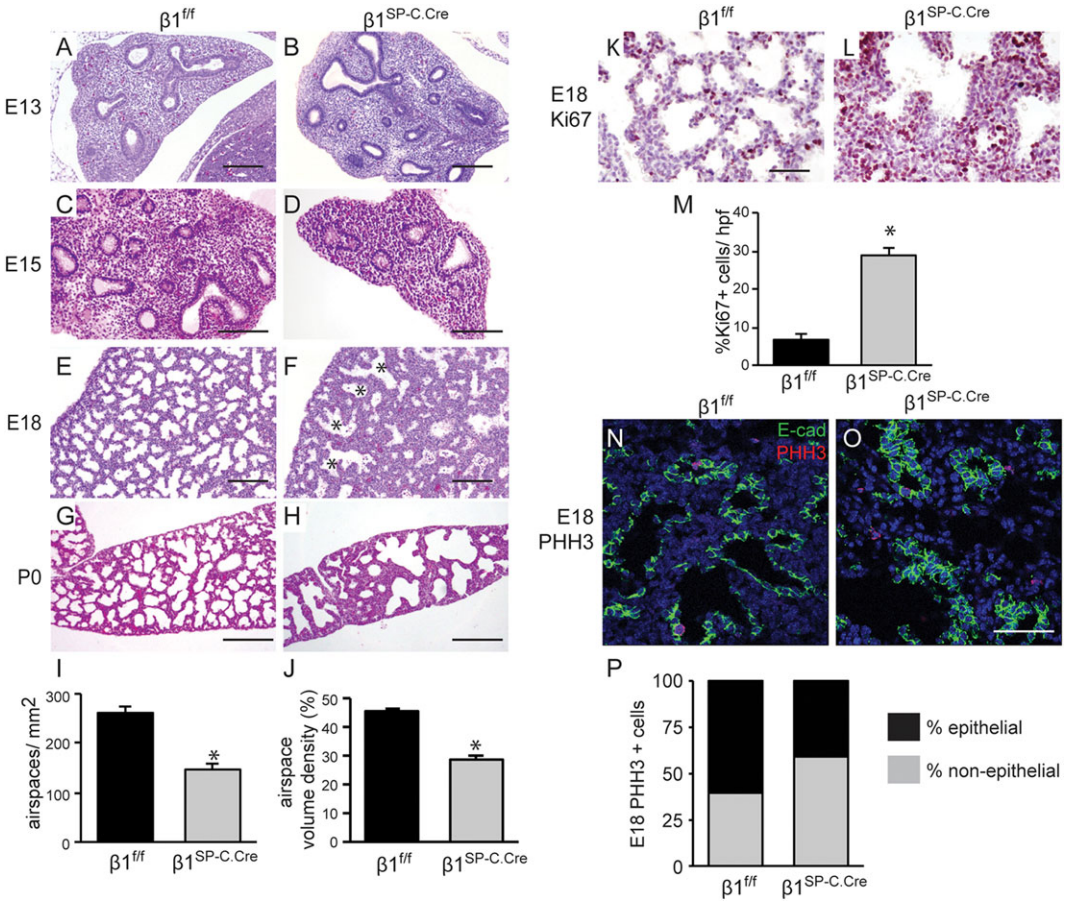

Fig. 3. Epithelial β1 integrin is required for lung branching morphogenesis. (A-H) H&E-stained paraffin sections of $\beta1^{f/f}$ (A,C,E,G) and $\beta1^{SP\text{-}C.Cre}$ (B,D,F,H) lungs. Decreased branching is present in E15, E18 and P0 $\beta1^{SP\text{-}C.Cre}$ lungs compared with $\beta1^{f/f}$ lungs. (F) Large airways near the lung periphery in E18 $\beta1^{SP\text{-}C.Cre}$ lungs (marked by asterisks). (I) Decreased number of airspaces per mm^2 in E18 $\beta1^{SP\text{-}C.Cre}$ lungs compared with $\beta1^{f/f}$ lungs (J) The airspace volume density was decreased in $\beta1^{SP\text{-}C.Cre}$ lungs (29±1%) compared with $\beta1^{f/f}$ lungs (46±1%). n=5 $\beta1^{SP\text{-}C.Cre}$ mice, n=3 $\beta1^{f/f}$ mice; five sections per mouse (I,J). (K,L) Ki67-stained E18 $\beta1^{SP\text{-}C.Cre}$ and $\beta1^{f/f}$ sections. (M) Quantification of Ki67+ cells per high-power field in E18 $\beta1^{SP\text{-}C.Cre}$ and $\beta1^{f/f}$ lungs. n=4 $\beta1^{SP\text{-}C.Cre}$ mice, n=3 $\beta1^{f/f}$ mice; six sections per mouse. (N,O) E18 $\beta1^{SP\text{-}C.Cre}$ and $\beta1^{f/f}$ sections immunostained for the mitotic marker phosphohistone H3 (PHH3) and the epithelial marker E-cadherin (E-cad). (P) The percentage of non-epithelial proliferation is increased in E18 $\beta1^{SP\text{-}C.Cre}$ lungs (58.7±0.5%) compared to $\beta1^{f/f}$ lungs (39.2±0.5%) (n=5 $\beta1^{SP\text{-}C.Cre}$ mice, n=4 $\beta1^{f/f}$ mice, seven sections per mouse). *P<0.05 between $\beta1^{SP\text{-}C.Cre}$ and $\beta1^{f/f}$ mice. Scale bars: 100 μm in A,B,E,F; 250 μm in C,D,G,H; in K, 50 μm for K,L.; in O, 50 μm for N,O.

β1 integrin plays a distinct role in lung alveolarization

To address whether the β1 integrin-dependent airway branching and alveolarization defects were separable, we generated triple transgenic mice (SP-C rtTA; tetO-Cre; $\beta1^{f/f}$) with a doxycycline-inducible lung epithelial-specific β1 integrin deletion at P0, which is after the completion of branching but prior to the start of alveologenesis. These mice retained the alveolarization defect seen in $\beta1^{SP\text{-}C.Cre}$ mice at P28, characterized by dilated airspaces, thickened alveolar septa, type II cell hyperplasia and increased alveolar macrophages (Fig. 7A-D). As seen in Fig. 7B, the subpleural airspaces in the peripheral lung were most severely affected, with more modest dilation of the proximal airspaces, consistent with proximal-distal maturation of the lung. These findings indicate that regulation of alveolarization by epithelial β1 integrin is independent of its role in branching morphogenesis.

Loss of epithelial β1 integrin results in lung inflammation which modulates lung alveolarization

An increase in alveolar macrophage numbers was confirmed in the bronchoalveolar lavage fluid (BALF) of 8-week-old $\beta1^{SP\text{-}C.Cre}$ mice (Fig. 8A-C). Increased macrophage accumulation, as measured by CD68 immunostaining, was seen as early as E18 in $\beta1^{SP\text{-}C.Cre}$ lungs (Fig. 8D-G); however, there were no difference in macrophage numbers in E15 $\beta1^{f/f}$ and $\beta1^{SP\text{-}C.Cre}$ lungs (supplementary material Fig. S1A,B). No differences in lung neutrophils or lymphocytes were identified between genotypes on immunostained lung sections (Fig. 8H-K).

The massive recruitment of macrophages, but not other types of immune or inflammatory cells, seen in adult $\beta1^{SP\text{-}C.Cre}$ lungs prompted us to investigate the contribution of increased alveolar macrophages to the alveolarization defect seen in $\beta1^{SP\text{-}C.Cre}$ mice. We therefore depleted macrophages during alveolarization by treating $\beta1^{f/f}$ and $\beta1^{SP\text{-}C.Cre}$ mice with intranasal clodronate from P5 to harvest at P14 or P28. Although clodronate-treated P28 $\beta1^{SP\text{-}C.Cre}$ mice still had airway branching defects (asterisks in Fig. 9B), this treatment rescued the alveolarization defect seen in $\beta1^{SP\text{-}C.Cre}$ mice. In contrast, P28 $\beta1^{SP\text{-}C.Cre}$ mice treated with vehicle (liposomes containing PBS) retained the phenotype of dilated airspaces, thickened alveolar septa, type II cell hyperplasia and increased alveolar macrophages (Fig. 9A-F). Normalization of the $\beta1^{SP\text{-}C.Cre}$ phenotype was quantified by measuring the average alveolar diameter (Fig. 9G) and quantification of secondary crests at P14 (Fig. 9H). Taken together, these data indicate that deficiency of β1 integrin disrupts alveolarization through recruitment and/or activation of macrophages.

Development (2014) 141, 4751-4762 doi:10.1242/dev.117200

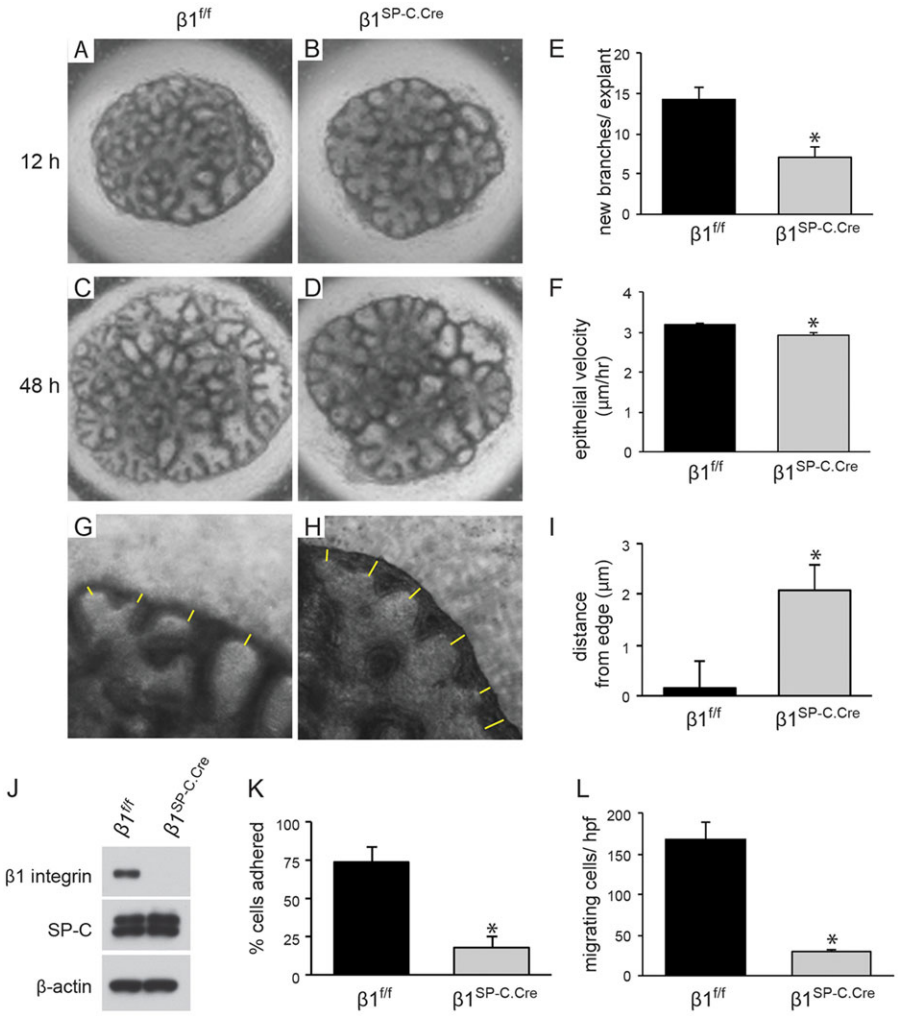

Fig. 4. Deleting β1 integrin in lung epithelium causes adhesion and migration defects. (A-D) E15 fetal lung explants have decreased branching after 48 h. (E) Quantification of new branches in $\beta1^{SP\text{-}C.Cre}$ explants compared to $\beta1^{f/f}$ explants (n=3 $\beta1^{SP\text{-}C.Cre}$ mice, n=6 $\beta1^{f/f}$ mice, five explants per mouse). (F) Outward epithelial velocity was decreased in $\beta1^{SP\text{-}C.Cre}$ explants compared with $\beta1^{f/f}$ explants over a 6 h time period (n=9 $\beta1^{SP\text{-}C.Cre}$ mice, n=5 $\beta1^{f/f}$ mice, one explant per mouse, ten consecutive airways per explant for F and I). (G-I) The distance from the epithelial edge to explant edge (yellow lines) was greater in $\beta1^{SP\text{-}C.Cre}$ compared with $\beta1^{f/f}$ explants. The difference is quantified in I. (J) Immunoblot for β1 integrin and SP-C on primary epithelial cell lysates showing epithelial-specific deletion in $\beta1^{SP\text{-}C.Cre}$ mice (blot representative of three separate experiments). (K) Decreased cell adhesion of isolated $\beta1^{SP\text{-}C.Cre}$ epithelial cells plated on laminin-511 compared with $\beta1^{f/f}$ epithelial cells (epithelial cells isolated from n=7 $\beta1^{SP\text{-}C.Cre}$ mice, n=6 $\beta1^{f/f}$ mice, completed in four separate assays, each performed in triplicate). (L) Isolated $\beta1^{SP\text{-}C.Cre}$ epithelial cells have decreased migration across a laminin-511-coated filter compared with $\beta1^{f/f}$ epithelial cells (n=6 from each group, completed in three separate assays, five sections analyzed per mouse). *P<0.05 between $\beta1^{SP\text{-}C.Cre}$ and $\beta1^{f/f}$ mice.

Given that inflammation that is predominantly mediated by macrophages impairs alveolarization in $\beta1^{SP\text{-}C.Cre}$ mice, we next sought to identify the mechanism of alveolar macrophage recruitment to the lungs of mice with epithelial β1 integrin deficiency. We first measured the BALF levels of the chemoattractant monocyte chemoattractant protein 1 (MCP-1; also known as CCL2), the major chemokine responsible for monocyte and macrophage recruitment. We found that MCP-1 levels were markedly increased in BALF from $\beta1^{SP\text{-}C.Cre}$ mice compared with control mice (438±52 pg/ml versus 142±5 pg/ml) (Fig. 10A). In contrast, there was no difference in the BALF levels of KC (also known as CXCL1), a neutrophil-specific chemoattractant (Fig. 10B). To determine whether the MCP-1 was derived from the epithelium, we measured MCP-1 levels in primary type II alveolar epithelial cells isolated from $\beta1^{f/f}$ and $\beta1^{SP\text{-}C.Cre}$ mice. As for BALF, levels of MCP-1, but not KC, were significantly increased in medium from $\beta1^{SP\text{-}C.Cre}$ epithelial cells compared with that from control $\beta1^{f/f}$ cells (Fig. 10C,D). These data suggest that intact β1 integrin suppresses the expression of chemokines in the lung epithelium.

MCP-1 expression has been previously shown to be induced by reactive oxygen species (ROS) in different cell types and disease states (Chen et al., 2004b; Lakshminarayanan et al., 2001; Vlahos et al., 2011; Xing and Remick, 2007a,b). To determine whether epithelial $\beta1^{SP\text{-}C.Cre}$ MCP-1 secretion was associated with an increase in ROS production, we performed both *in vivo* and *in vitro* ROS assays. *In vivo*, we assayed in lungs of $\beta1^{SP\text{-}C.Cre}$ and control mice for ROS production by bioluminescence imaging following injection of a modified luminol derivative (Han et al., 2013). We found increased ROS production over the chest of $\beta1^{SP\text{-}C.Cre}$ mice compared with $\beta1^{f/f}$ control mice (Fig. 10E-G). To define whether the β1 integrin-deficient epithelium directly contributed to ROS production, we examined epithelial lipid peroxidation, as an indicator of oxidative stress. Primary type II alveolar epithelial cells isolated from $\beta1^{SP\text{-}C.Cre}$ mice had a fivefold increase in lipid peroxidation over $\beta1^{f/f}$ epithelial cells (Fig. 10H). These findings suggest that deleting β1 integrin in epithelial cells alters ROS production, which in turn regulates macrophage influx.

DISCUSSION

We found that deleting β1 integrin in lung epithelium beginning at E10.5 results in abnormal lung development with mortality by 4 months of age. A variety of specific defects were identified, including altered branching morphogenesis, impaired alveolarization with epithelial cell differentiation defects and persistent macrophage-mediated inflammation, indicating that β1 integrin expression in the lung epithelium plays multiple roles in distinct phases of lung development.

Our findings are complementary to a prior study that found that epithelial depletion of β1 integrin beginning at E9.5 causes a serious branching defect and neonatal death (Chen and Krasnow, 2012).

Development (2014) 141, 4751-4762 doi:10.1242/dev.117200

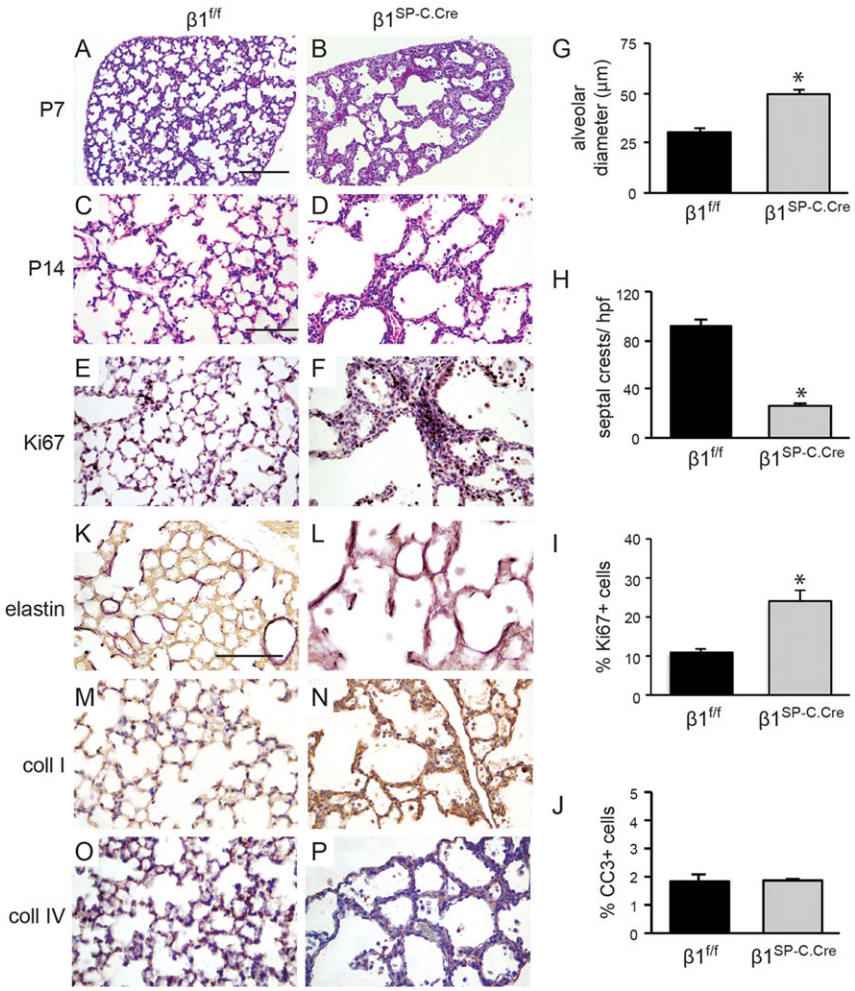

Fig. 5. Loss of β1 integrin results in alveolarization defects. (A-D) H&E-stained paraffin sections of $\beta1^{f/f}$ (A,C) and $\beta1^{SP\text{-}C.Cre}$ (B,D) lungs. Decreased alveolar septation is seen in P7 (B) and P14 $\beta1^{SP\text{-}C.Cre}$ lungs (D). (E,F) Increased Ki67 staining in P14 $\beta1^{SP\text{-}C.Cre}$ lungs. (G,H) Increased alveolar diameter (G) and secondary crests per high-power field (H) in P14 $\beta1^{SP\text{-}C.Cre}$ lungs (n=5 $\beta1^{SP\text{-}C.Cre}$ mice, n=4 $\beta1^{f/f}$ mice, five sections per mouse). (I) $\beta1^{SP\text{-}C.Cre}$ alveolar septa have increased Ki67+ cells compared with $\beta1^{f/f}$ lungs (n=3 mice for each group, six sections per mouse). (J) There was no difference in the number of cleaved caspase-3-positive (CC3+) cells between P14 $\beta1^{SP\text{-}C.Cre}$ and $\beta1^{f/f}$ lungs (n=5 $\beta1^{SP\text{-}C.Cre}$ mice, n=6 $\beta1^{f/f}$ mice, ten sections per mouse). (K-P) Immunostaining for elastin, collagen I, and collagen IV on P14 $\beta1^{SP\text{-}C.Cre}$ (L,N,P) and $\beta1^{f/f}$ (K,M,O) paraffin sections. Scale bars: in A, 250 μm for A,B; in C, 100 μm for C-F); in K, 50 μm for K-P. *P<0.05 between $\beta1^{SP\text{-}C.Cre}$ and $\beta1^{f/f}$ mice.

Although the disparity in these phenotypes could be due to differences in potency between the Cre-expressing mice (Shh and the SP-C), it is more likely that β1 integrin has a more profound role in early rather than late lung development. This is consistent with the crucial role for β1 integrin in the early development of other branched organs. In the kidney, β1 integrin deletion at initiation (E10.5) of ureteric bud development results in a lethal phenotype but has no effect when it is removed at E18.5 (Zhang et al., 2009). In addition, fetal β1 deletion in the basal epithelial cells in the mammary gland causes a branching defect, whereas postpubertal deletions do not (Faraldo et al., 1997; Naylor et al., 2005; Taddei et al., 2008). Thus, epithelial cell β1 integrin expression appears to be a crucial requirement for early embryonic development of branched organs.

In contrast to our findings, mice with epithelial-targeted deficiency of the integrin α3 subunit have a normal lifespan, preserved alveolar architecture and no differences in total lung capacity and airway resistance (Kim et al., 2009). These mice have only mild type II alveolar epithelial cell hyperplasia, mild fibrosis and increased numbers of macrophages in BALF (Kim et al., 2009). In contrast to the epithelial-specific α3-null mice, global integrin α3 deletion results in an airway branching defect (Kreidberg et al., 1996), and mice mutant for both integrin α3 and α6 die at E16 with a single-lobed right lung and an almost absent left lung (De Arcangelis et al., 1999). Consistent with findings in constitutive integrin α3-null mice, functional mutations of integrin α3 in humans cause pulmonary hypoplasia, severe fibrosis with thickened alveolar septa lined with reactive type II pneumocytes, and increased numbers of alveolar macrophages (Has et al., 2012; Nicolaou et al., 2012). Although integrins expressed by the epithelial and mesenchymal compartments of the lung probably play distinct roles in different aspects of lung development, available information suggests that several of the α-β1 integrin heterodimers expressed in lung epithelium regulate lung branching morphogenesis and alveolarization.

We show that integrin β1-null type II alveolar epithelial cells are increased in number and morphologically abnormal with enlarged nuclei and fewer mitochondria and lamellar bodies, suggesting abnormal type II alveolar epithelial cell differentiation. Consistent with this abnormal morphology, the epithelial cells lining dilated airspaces in $\beta1^{SP\text{-}C.Cre}$ lungs are positive for both type I and type II cell markers at P14. These cells appear similar to the bipotent epithelial progenitors cells recently identified during late embryonic lung development (Yamashita et al., 2004), suggesting that β1 integrin is required for normal alveolar epithelial cell differentiation. Abnormal epithelial morphology is also seen in constitutive integrin α3-null mice (Kreidberg et al., 1996) and lung epithelial-specific laminin α5-null mice (Nguyen et al., 2005). Different *in vitro* ECM culture conditions have been shown to alter lung epithelial cell differentiation with laminins promoting a type II cell phenotype, and fibronectin and collagen I inducing type I cell characteristics (Isakson et al., 2001; Lwebuga-Mukasa, 1991; Olsen et al., 2005; Rannels and Rannels, 1989). In addition to the ECM type, physical force mediated

Development (2014) 141, 4751-4762 doi:10.1242/dev.117200

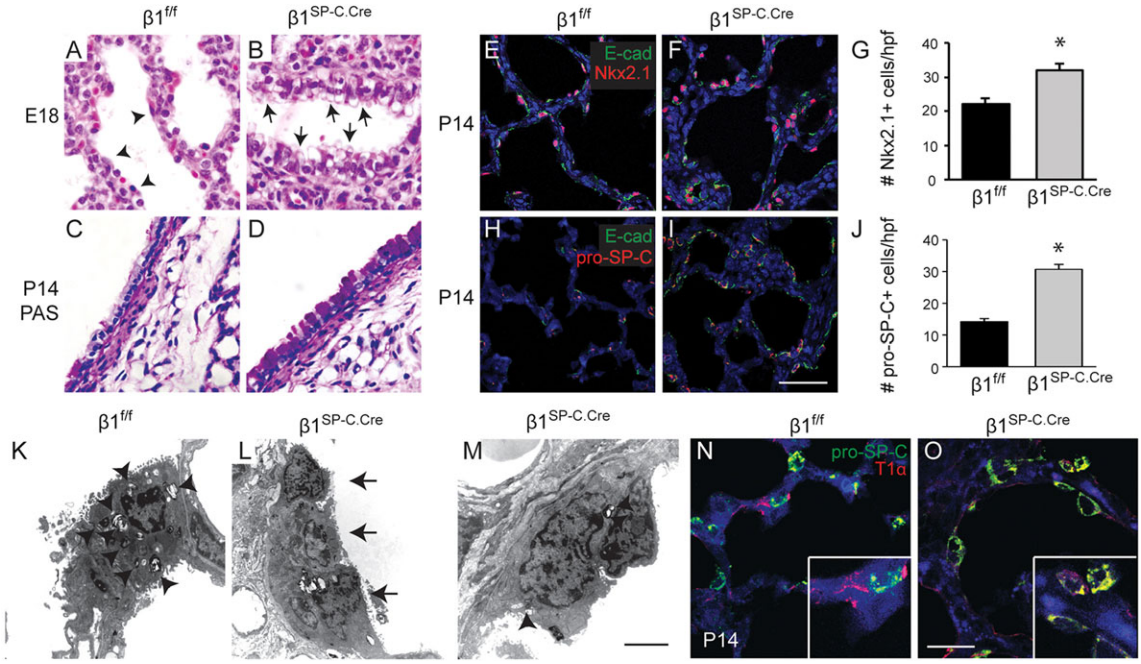

Fig. 6. β1$^{SP\text{-}C.Cre}$ mice have defects in proximal and distal epithelial differentiation. (A,B) Cuboidal epithelial cells (arrows) seen in E18 β1$^{SP\text{-}C.Cre}$ H&E-stained lungs. Flattened epithelium (arrowheads) seen in E18 β1$^{f/f}$ lungs. (C,D) Increase in periodic acid schiff (PAS)-positive epithelial cells in β1$^{SP\text{-}C.Cre}$ lungs at P14. (E,F) Immunostaining for the type II cell marker Nkx2.1 (red) and E-cadherin (green). (G) The number of Nkx2.1+ cells in β1$^{SP\text{-}C.Cre}$ lungs was greater than in β1$^{f/f}$ lungs (n=5 β1$^{SP\text{-}C.Cre}$ mice, n=5 β1$^{f/f}$ mice, eight sections per mouse). (H,I) Immunostaining for type II cell marker SP-C (red) and E-cadherin (green). (J) The number of SP-C+ cells in β1$^{SP\text{-}C.Cre}$ lungs was greater than in β1$^{f/f}$ lungs (n=4 β1$^{SP\text{-}C.Cre}$ mice, n=4 β1$^{f/f}$ mice, eight sections per mouse). (K-M) Paucity of lamellar bodies (arrowheads) in β1$^{SP\text{-}C.Cre}$ type II cells as assessed in transmission electron microscopy images (taken at 11,000×). Type II cell (arrows) hyperplasia along thickened alveolar septa in β1$^{SP\text{-}C.Cre}$ mice (L). (N,O) Dual positive epithelial cells are seen in β1$^{SP\text{-}C.Cre}$ lungs, demonstrated by 63× confocal images of co-immunostaining for the type I marker T1α (red) and type II marker pro-SP-C (green). Insets are 100× images. *P≤0.05 between β1$^{SP\text{-}C.Cre}$ and β1$^{f/f}$ mice. Scale bars: in I, 50 μm for E,F,H,I; in M, 2 μm for K-M; in O, 25 μm for N,O.

through integrin-ECM interactions regulate lung epithelial cell differentiation *in vitro* through unknown mechanisms (Huang et al., 2012; Sanchez-Esteban et al., 2004; Wang et al., 2013, 2006, 2009). Thus, it is likely that abnormally differentiated type II cells in β1$^{SP\text{-}C.Cre}$ mice result from impaired integrin-dependent attachment and altered interactions with the ECM. This explanation is consistent with abnormalities in epithelial cell differentiation induced by deletion of integrin β1 in other organs, such as the kidney proximal tubule (Elias et al., 2014), enterocytes (Jones et al., 2006), keratinocytes (Brakebusch et al., 2000), mammary epithelium (Naylor et al., 2005) and the submandibular gland (Menko et al., 2001).

Many studies have focused on the role of mesenchymal growth factors and epithelial receptor signaling in lung development, and there are many similarities between mice with growth factor and/or receptor deletions and mice lacking β1 integrin in the lung epithelium. Lungs from FGF10- and FGFR2-null mice fail to branch beyond the trachea (Min et al., 1998;

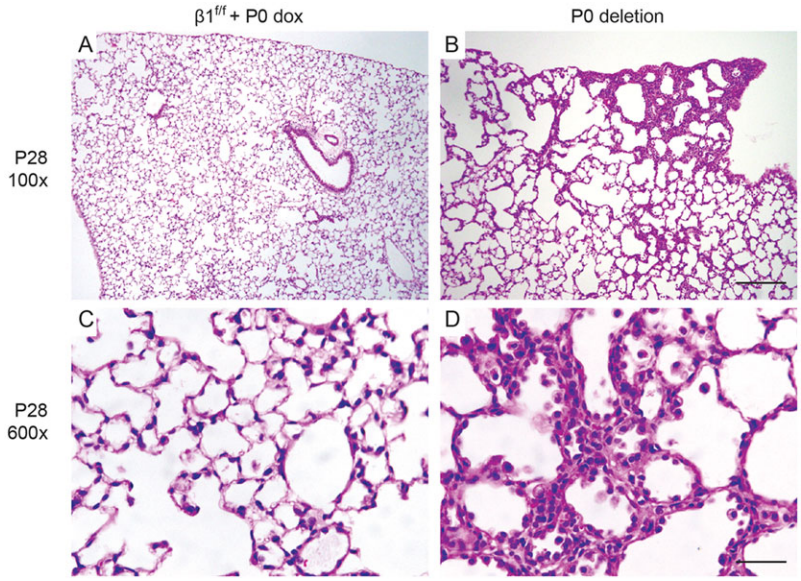

Fig. 7. Lung epithelial β1 integrin deletion at P0 retains alveolarization defect. (A-D) H&E-stained paraffin sections of P28 SP-C rtTA; tetO-Cre; β1$^{f/f}$ (B,D) and littermate β1$^{f/f}$ (A,C) lungs from mice given doxycycline (dox)-containing drinking water from P0 to P28. Mice with a lung epithelial β1 integrin deletion induced at P0 have an alveolarization defect similar to β1$^{SP\text{-}C.Cre}$ mice. Representative low magnification (taken at ×100) images are shown in A,B, and high-magnification (taken at ×600) images in C,D. Scale bars: in B, 250 μm for A,B; in D, 25 μm for C,D.

Development (2014) 141, 4751-4762 doi:10.1242/dev.117200

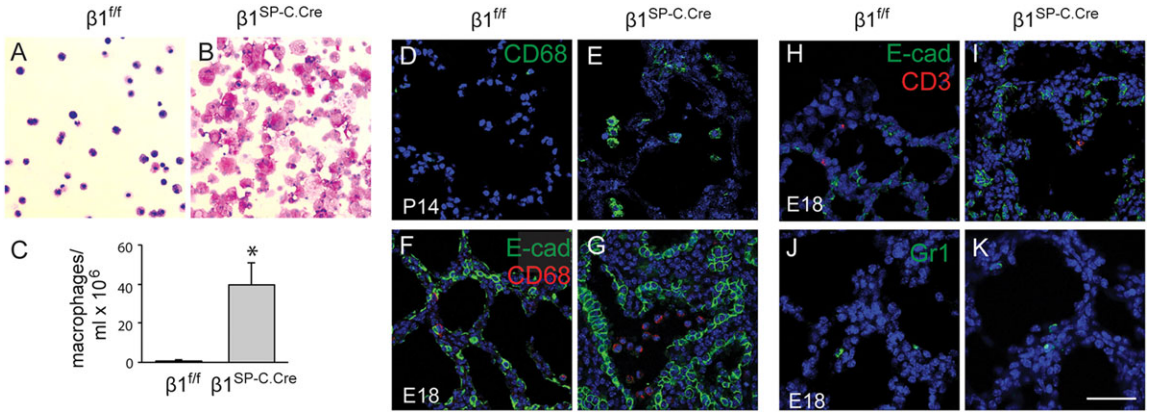

Fig. 8. β1$^{SP\text{-}C.Cre}$ mice have increased alveolar macrophages. (A,B) Microscopy of cytospin from β1$^{SP\text{-}C.Cre}$ and β1$^{f/f}$ mice. (C) The increased number of macrophages in β1$^{SP\text{-}C.Cre}$ BALF was quantified (*n*=4 mice in each group). (D,E) P14 frozen sections immunostained for CD68 (green). (F,G) E18 frozen sections immunostained for CD68 (red) and E-cadherin (green). (H,I) E18 frozen sections immunostained for CD3 (red). (J,K) E18 frozen sections immunostained for Gr1 (green). **P*<0.05 between β1$^{SP\text{-}C.Cre}$ and β1$^{f/f}$ mice. Scale bar: in K, 50 µm for D-K.

Sekine et al., 1999), FGFR3/4-null mice have an alveolarization defect (Weinstein et al., 1998), and mice null for both FGFR3 and FGFR4 have a mild branching defect and thickened alveolar septa, similar to the β1$^{SP\text{-}C.Cre}$ mice (Miettinen et al., 1995). We have previously shown in the kidney that β1 integrin is required for FGF2 and FGF10 signaling in ureteric bud development (Zhang et al., 2009), and that β1 integrin regulates FGF- and EGF-dependent signaling in renal collecting duct cells (Mathew et al., 2012). Thus many of the phenotypical characteristics observed in the β1$^{SP\text{-}C.Cre}$ mice might be caused by both alterations in integrin-dependent growth factor signaling as well as adhesion and migration defects.

Our studies point to an important role for β1 integrin in maintaining alveolar homeostasis, which is required for normal alveolarization during the early post-natal period. In the mammary gland, epithelial β1 integrin deletion results in epithelial detachment from the basement membrane without inflammation (Li et al., 2005; Naylor et al., 2005). In contrast, increased numbers of macrophages were observed in the lungs of mice with laminin α3 chain mutations (Urich et al., 2011) and in the lungs of humans with integrin α3 mutations (Nicolaou et al., 2012), suggesting that β1 integrin-mediated regulation of inflammation is specific to the lung epithelium. Whereas β1 integrin deficiency results in increased ROS production and MCP-1 secretion from alveolar

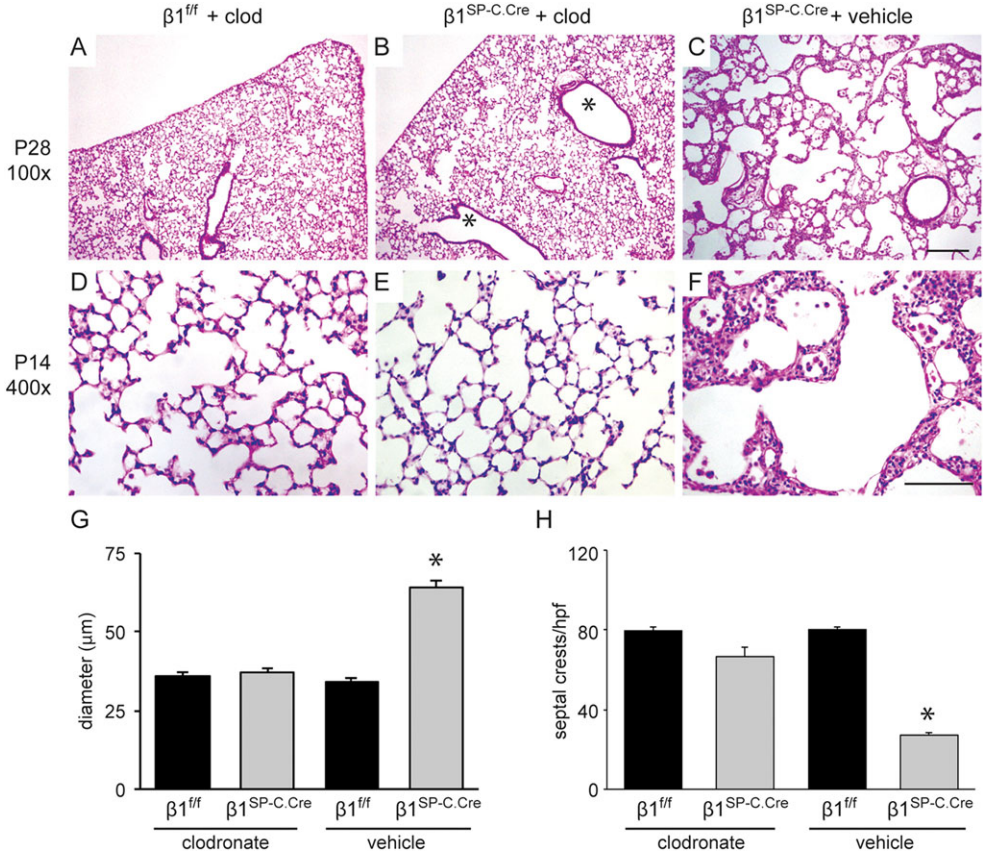

Fig. 9. Macrophage depletion rescues alveolarization defect in β1$^{SP\text{-}C.Cre}$ mice. (A-F) H&E-stained paraffin sections of clodronate-treated β1$^{f/f}$ lungs (A,D) and β1$^{SP\text{-}C.Cre}$ lungs treated with either clodronate (B,E) or lipid vehicle (C,F), harvested at P28 (A-C) and P14 (D-F). Lungs from clodronate-treated β1$^{SP\text{-}C.Cre}$ mice (B,E) have normal septation but demonstrate a branching defect with large airways that fail to taper at the lung periphery (asterisks in B), whereas vehicle-treated β1$^{SP\text{-}C.Cre}$ lungs retain the original β1$^{SP\text{-}C.Cre}$ phenotype (C,F). (G,H) Lung morphometry on P14 H&E-stained sections. Alveolar diameter (G) and number of secondary crests per high-power field (H) in P14 β1$^{SP\text{-}C.Cre}$ lungs are normalized to the levels in β1$^{f/f}$ with depletion of macrophages from P5 to P14 (*n*=4 β1$^{SP\text{-}C.Cre}$ mice, *n*=4 β1$^{f/f}$ mice, six sections per mouse). **P*<0.05 between vehicle-treated β1$^{SP\text{-}C.Cre}$ mice and each of the other groups. Scale bars: in C, 250 µm for A-C; in F, 100 µm for D-F.

Development (2014) 141, 4751-4762 doi:10.1242/dev.117200

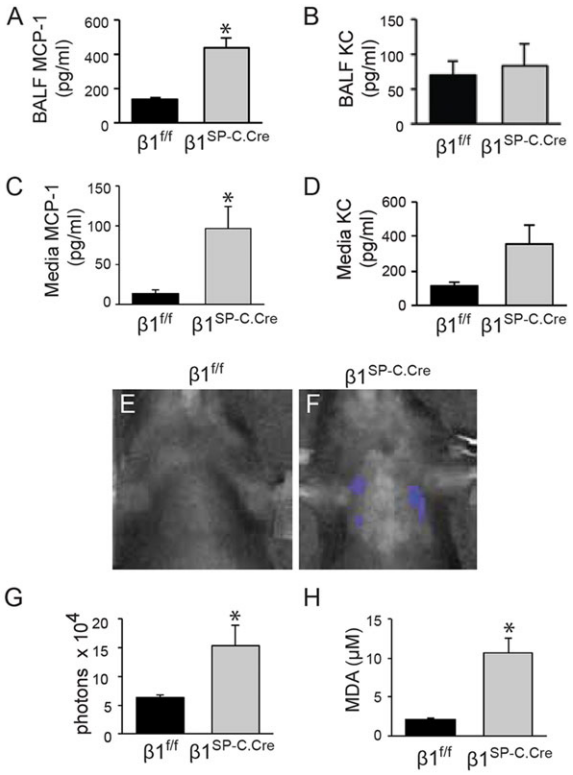

Fig. 10. Deletion of β1 integrin in lung epithelial cells results in increased epithelial MCP-1 secretion and ROS production. (A) $\beta1^{SP\text{-}C.Cre}$ BALF had significantly increased MCP-1 compared with $\beta1^{f/f}$ BALF as measured by ELISA (n=3 $\beta1^{SP\text{-}C.Cre}$, n=4 $\beta1^{f/f}$ BALF). (B) ELISA for KC, a neutrophil chemoattractant, was similar between $\beta1^{SP\text{-}C.Cre}$ and $\beta1^{f/f}$ BALF (n=4 for each group). (C) MCP-1 was significantly increased in medium collected from isolated $\beta1^{SP\text{-}C.Cre}$ epithelial cells compared with that from $\beta1^{f/f}$ epithelial cells (n=5 per group for C and D). (D) Levels of KC was increased in $\beta1^{SP\text{-}C.Cre}$ epithelial cell medium, but the difference was not significant (P=0.14). (E,F) *In vivo* bioluminescence assay shows increased ROS production (purple) in the thorax of $\beta1^{SP\text{-}C.Cre}$ mice. (G) The photon emission from the ROS bioluminescence assay in $\beta1^{SP\text{-}C.Cre}$ mice (n=3 $\beta1^{SP\text{-}C.Cre}$ mice, n=8 $\beta1^{f/f}$ mice). *P<0.05 between $\beta1^{SP\text{-}C.Cre}$ and $\beta1^{f/f}$ mice.

epithelial cells, the molecular mechanisms accounting for these findings will require further study. Increased ROS production has been described in integrin α1-null glomerular mesangial cells (Chen et al., 2007); however, this has not previously been shown to occur in epithelial cells, and β1 integrins have not been linked to MCP-1 expression or ROS production in other systems. Although the role of macrophages during alveolarization is not well understood, we and others have shown that macrophages and macrophage-derived products disrupt branching morphogenesis (Blackwell et al., 2011; Nold et al., 2013). Specifically, we have found that products of activated macrophages can impair expression of molecules by epithelial and mesenchymal cells that are important for control of airway branching, including BMP4, Wnt7b and FGF10 (Benjamin et al., 2010; Blackwell et al., 2011; Carver et al., 2013). We speculate that mediators secreted by activated macrophages might also disrupt crucial epithelial-mesenchymal interactions required for normal septation and remodeling of the interstitium.

In conclusion, this study shows that β1 integrin expression in lung epithelium is required during different stages of lung development for airway branching morphogenesis, alveolarization and maintenance of homeostasis. In addition to its well-known functional role in epithelial cell adhesion and migration, β1 integrin modulates alveolar cell differentiation and alveolar septal ECM deposition. Finally, we have also shown that β1 integrin regulates epithelial chemokine and ROS production, which appears to be a new mechanism whereby cell-ECM interactions regulate lung inflammation and alveolarization.

MATERIALS AND METHODS

Generation of $\beta1^{SP\text{-}C.Cre}$ mice

All experiments were approved by the Vanderbilt University Institutional Animal Use and Care Committee. Transgenic mice expressing Cre recombinase under control of the surfactant protein C promoter (SP-C-Cre) were generated by Brigid Hogan (Duke University, Durham, NC, USA) (Okubo et al., 2005) and integrin $\beta1^{flox/flox}$ mice were a generous gift from Elaine Fuchs (Howard Hughes Medical Institute, The Rockefeller University, New York, NY) (Raghavan et al., 2000). $\beta1^{SP\text{-}C.Cre}$ mice (C57BL/6J background) were generated by crossing a male heterozygote (SP-C-Cre; $\beta1^{f/WT}$) with a female control ($\beta1^{f/f}$). This mating strategy deletes β1 integrin specifically from the lung epithelium from E10.5 in SP-C-Cre; $\beta1^{f/f}$ mice (called $\beta1^{SP\text{-}C.Cre}$ mice). Littermate $\beta1^{f/f}$ mice were used as controls.

Generation of inducible β1 integrin deletion

Triple transgenic mice (SP-C rtTA; tetO-Cre; $\beta1^{f/f}$) were obtained by breeding (Perl et al., 2002; Tanjore et al., 2013) and lung epithelial-specific deletion of β1 integrin was induced by the ingestion of doxycycline in the drinking water (2 g/dl). $\beta1^{f/f}$ littermates given identical dosage of doxycycline were used as controls.

Morphological analysis

Lungs were dried overnight at 75°C. Non-anesthetized oxygen saturations were obtained using MouseOx pulse oxymetry (Starr Life Sciences, Holliston, MA). Lungs were embedded, sectioned and stained as indicated. Ki67 staining was used for analysis of proliferation (Abcam ab16667, Cambridge, MA). Lung morphometry was performed on images viewed using a 40× objective for six sections per mouse, with a minimum of four mice in each group (Kauffman, 1977) using Image Pro Plus software. The airspace volume density was measured by dividing the sum of the airspace area by the total area. P14 alveolar secondary crests were quantified as previously described (Nicola et al., 2009). For electron microscopy, adult lungs were processed, post-fixed with potassium ferrous cyanide, dehydrated with graded acetone, sectioned at 1 µm and imaged using a Philips FEI T-12 transmission electron microscope.

Lung explants

Lung explants from E15 $\beta1^{SP\text{-}C.Cre}$ and $\beta1^{f/f}$ mice were cultured on permeable supports and on an air-liquid interface at 37°C in 95% air with 5% CO_2 overnight to allow adherence to the filter, as previously described (Blackwell et al., 2011; Prince et al., 2005; Prince et al., 2004). Peripheral branch counts (all branches touching the edge of the explant) were obtained from images taken at 12 and 48 h in culture using a Leica DFC450 microscope. Time-lapse images were obtained every 10 min for 8 h using a Nikon Ti Eclipse microscope. The epithelial edge was tracked on the first ten consecutive peripheral airways from the 12:00 position using ImageJ analysis software.

Depletion of macrophages with clodronate

Clodronate (dichloromethylene diphosphonic acid; Sigma-Aldrich) and sterile PBS-containing liposomes (vehicle) were prepared as previously described (Everhart et al., 2005; Zaynagetdinov et al., 2011). $\beta1^{f/f}$ and $\beta1^{SP\text{-}C.Cre}$ mice were treated with intranasal clodronate or PBS-containing liposome vehicle every 5 days from P5 until harvest at P14 or P28. Intranasal clodronate was given at doses of 12 µl, 15 µl, 18 µl, 21 µl and 24 µl at P5, P10, P15, P20 and P25, respectively. Duplicate experiments were performed using PBS-containing liposome vehicle control.

Immunostaining

For immunofluorescence, 8 µm frozen sections were fixed with 10% formalin for 20 min at room temperature, permeabilized with 0.1% Triton X-100, blocked in 5% donkey serum in PBS, and stained with the

Development (2014) 141, 4751-4762 doi:10.1242/dev.117200

following primary antibodies: anti-β1 integrin (1:250, Millipore MAB1997), anti-E-cadherin (1:500, Invitrogen 131900), anti-cleaved caspase 3 (1:500, Cell Signaling 9661), anti-Nkx2.1 (1:250, Santa Cruz Biotechnology sc-13040), anti-pro-SP-C (1:500, Abcam ab90716), anti-T1α (1:250, Developmental Studies Hybridoma Bank 8.1.1), anti-CD68 (1:500, Abcam ab53444), anti-CD31 (1:500, BD Pharmingen 550274), anti-CD3 (1:500, Abcam ab5690) and FITC-conjugated anti-Gr1 (also known as Gsr; 1:500, eBioscience 11-5931) antibodies. Detection of bound antibodies was accomplished with Alexa Fluor 488-conjugated donkey anti-rat IgG or Alexa Fluor 555-conjugated donkey anti-rabbit IgG (both 1:500, Life Technologies A31572). Slides were analyzed using a Leica SPE confocal microscope.

Isolation of type II epithelial cells and collection of conditioned medium

Type II epithelial cells were isolated from P28 $\beta1^{SP\text{-}C.Cre}$ and $\beta1^{f/f}$ mice as previously described, yielding >90% type II cells (Rice et al., 2002; Young et al., 2012). Tissue was digested using dispase and the epithelial cell population was separated from leukocyte and monocyte populations using antibody-coated plates (CD45 and CD32, BD Pharmingen) for negative selection. After incubation for 2 h at 37°C in 5% CO_2, type II cells were harvested, centrifuged and were resuspended in lysis buffer or cultured. Conditioned medium was collected at 24 h from 10^6 isolated epithelial cells per well cultured in serum-free medium on laminin-511.

Cell adhesion and migration assays

Cell adhesion and migration assays were performed with isolated epithelial cells from $\beta1^{SP\text{-}C.Cre}$ and $\beta1^{f/f}$ mice in serum-free bronchial epithelial growth medium (BEGM) (Chen et al., 2004a). Plates and filters were coated with purified laminin 511 (1 µg/ml, made by Eugenia Yazlovitskaya), a prominent lung basement membrane component, which we purified from HEK cells stably transfected with the α5β1γ1 using methods previously described (McKee et al., 2009).

For the adhesion assay, 10^5 cells were added per well, and cells that were adherent at 6 h were fixed, stained with Crystal Violet and solubilized. The optical density was read at 540 nm. Each mouse was analyzed in triplicate and five independent experiments were averaged. For the migration assay, 2×10^5 cells were added to the upper chamber of a filter. After 6 h, cells that migrated through the filter were stained and counted. Five random fields were analyzed and three independent experiments were performed.

Bronchoalveolar lavage

Sterile saline lavages were performed with 35 µl/g of PBS after killing, using a 20 g blunt-tipped needle inserted into the trachea. Samples were centrifuged at 400 ***g*** for 10 min, and the supernatant was collected. Cell counts were performed using a Bio-Rad TC10 Automated Cell Counter.

Immunoblotting

Total protein (40 µg) collected from isolated type II cell lysate was electrophoresed in a 10% gel and transferred onto nitrocellulose membranes. Membranes were blocked and incubated with different primary antibodies [anti-SP-C (1:5000, Abcam 90716), anti-β1 integrin from Millipore (1:10,000, 1952) and anti-β-actin (1:5000, Sigma A5316) antibodies], followed by the appropriate horseradish peroxidase (HRP)-conjugated secondary antibodies. Immunoreactive bands were identified using enhanced chemiluminescence according to the manufacturer's instructions.

Enzyme-linked immunosorbent assay

Enzyme-linked immunosorbent assay (ELISA) for MCP-1 and KC on BALF and medium was performed according to the manufacturer's instructions (R&D Systems, MJE00 and MKC00B, respectively). Each sample was run in triplicate.

Thiobarbituric acid reactive substances assay

Lipid peroxidation in freshly isolated epithelial cells from $\beta1^{SP\text{-}C.Cre}$ and $\beta1^{f/f}$ mice was detected by measuring the reaction of thiobarbituric acid with malondialdehyde colorimetrically at 540 nm (Cayman Chemical Company).

In vivo ROS assay

ROS production was detected in $\beta1^{SP\text{-}C.Cre}$ and $\beta1^{f/f}$ mice *in vivo* as previously described (Han et al., 2013). L-012 (Wako Chemicals), a luminol analog, was injected retro-orbitally. Upon reaction with superoxide, luminescence was produced and detected by an IVIS system device (Xenogen). Luminescence data was collected using Living Image software v.4.1 (Xenogen).

Statistics

The Student's *t*-test was used for comparisons between two groups with results representing mean±s.e.m. $P<0.05$ was considered statistically significant.

Acknowledgements

We thank Brigid Hogan, Elaine Fuchs and Eugenia Yazlovitskaya for generously supplying reagents.

Competing interests

The authors declare no competing financial interests.

Author contributions

E.J.P., L.R.Y., L.S.P., T.S.B. and R.Z. developed the concepts, performed experiments and data analysis, and prepared or edited the manuscript prior to submission. P.M.G., V.V.P., R.Z., J.T.B., A.M.I., R.v.d.M., L.A.G., N.B. and W.H. performed experiments for the manuscript.

Funding

This work was in part supported by the Veterans Affairs Merit Reviews to T.S.B. and R.Z. [1I01BX002196-01]; by the National Institutes of Health [DK069221 and DK083187 to R.Z., HL092870 and HL085317 to T.S.B., HL097195 and HL116358 to L.S.P. and T.S.B., HL086324 to L.S.P.]. Deposited in PMC for release after 12 months.

Supplementary material

Supplementary material available online at
http://dev.biologists.org/lookup/suppl/doi:10.1242/dev.117200/-/DC1

References

Benjamin, J. T., Gaston, D. C., Halloran, B. A., Schnapp, L. M., Zent, R. and Prince, L. S. (2009). The role of integrin alpha8beta1 in fetal lung morphogenesis and injury. *Dev. Biol.* **335**, 407-417.

Benjamin, J. T., Carver, B. J., Plosa, E. J., Yamamoto, Y., Miller, J. D., Liu, J.-H., van der Meer, R., Blackwell, T. S. and Prince, L. S. (2010). NF-kappaB activation limits airway branching through inhibition of Sp1-mediated fibroblast growth factor-10 expression. *J. Immunol.* **185**, 4896-4903.

Blackwell, T. S., Hipps, A. N., Yamamoto, Y., Han, W., Barham, W. J., Ostrowski, M. C., Yull, F. E. and Prince, L. S. (2011). NF-kappaB signaling in fetal lung macrophages disrupts airway morphogenesis. *J. Immunol.* **187**, 2740-2747.

Brakebusch, C., Grose, R., Quondamatteo, F., Ramirez, A., Jorcano, J. L., Pirro, A., Svensson, M., Herken, R., Sasaki, T., Timpl, R. et al. (2000). Skin and hair follicle integrity is crucially dependent on beta 1 integrin expression on keratinocytes. *EMBO J.* **19**, 3990-4003.

Cardoso, W. V. and Lü, J. (2006). Regulation of early lung morphogenesis: questions, facts and controversies. *Development* **133**, 1611-1624.

Carver, B. J., Plosa, E. J., Stinnett, A. M., Blackwell, T. S. and Prince, L. S. (2013). Interactions between NF-kappaB and SP3 connect inflammatory signaling with reduced FGF-10 expression. *J. Biol. Chem.* **288**, 15318-15325.

Chen, J. and Krasnow, M. A. (2012). Integrin Beta 1 suppresses multilayering of a simple epithelium. *PLoS ONE* **7**, e52886.

Chen, D., Roberts, R., Pohl, M., Nigam, S., Kreidberg, J., Wang, Z., Heino, J., Ivaska, J., Coffa, S., Harris, R. C. et al. (2004a). Differential expression of collagen- and laminin-binding integrins mediates ureteric bud and inner medullary collecting duct cell tubulogenesis. *Am. J. Physiol. Renal Physiol.* **287**, F602-F611.

Chen, X.-L., Zhang, Q., Zhao, R. and Medford, R. M. (2004b). Superoxide, H2O2, and iron are required for TNF-alpha-induced MCP-1 gene expression in endothelial cells: role of Rac1 and NADPH oxidase. *Am. J. Physiol. Heart Circ. Physiol.* **286**, H1001-H1007.

Chen, X., Abair, T. D., Ibanez, M. R., Su, Y., Frey, M. R., Dise, R. S., Polk, D. B., Singh, A. B., Harris, R. C., Zent, R. et al. (2007). Integrin alpha1beta1 controls reactive oxygen species synthesis by negatively regulating epidermal growth factor receptor-mediated Rac activation. *Mol. Cell. Biol.* **27**, 3313-3326.

De Arcangelis, A., Mark, M., Kreidberg, J., Sorokin, L. and Georges-Labouesse, E. (1999). Synergistic activities of alpha3 and alpha6 integrins are required during apical ectodermal ridge formation and organogenesis in the mouse. *Development* **126**, 3957-3968.

Development (2014) 141, 4751-4762 doi:10.1242/dev.117200

Elias, B. C., Mathew, S., Srichai, M. B., Palamuttam, R., Bulus, N., Mernaugh, G., Singh, A., Sanders, C. R., Harris, R. C., Pozzi, A. et al. (2014). The integrin beta 1 subunit regulates paracellular permeability of kidney proximal tubule cells. *J. Biol. Chem.* 289, 8532-8544.

Everhart, M. B., Han, W., Parman, K. S., Polosukhin, V. V., Zeng, H., Sadikot, R. T., Li, B., Yull, F. E., Christman, J. W. and Blackwell, T. S. (2005). Intratracheal administration of liposomal clodronate accelerates alveolar macrophage reconstitution following fetal liver transplantation. *J. Leukoc. Biol.* **77**, 173-180.

Faraldo, M. M., Deugnier, M.-A., Thiery, J.-P. and Glukhova, M. A. (1997). Beta 1-integrins in the mammary gland development. *Mol. Biol. Cell* **8**, 182a.

Georges-Labouesse, E., Messaddeq, N., Yehia, G., Cadalbert, L., Dierich, A. and Le Meur, M. (1996). Absence of integrin alpha 6 leads to epidermolysis bullosa and neonatal death in mice. *Nat. Genet.* **13**, 370-373.

Han, W., Li, H., Cai, J., Gleaves, L. A., Polosukhin, V. V., Segal, B. H., Yull, F. E. and Blackwell, T. S. (2013). NADPH oxidase limits lipopolysaccharide-induced lung inflammation and injury in mice through reduction-oxidation regulation of NF-kappaB activity. *J. Immunol.* **190**, 4786-4794.

Has, C., Spartà, G., Kiritsi, D., Weibel, L., Moeller, A., Vega-Warner, V., Waters, A., He, Y., Anikster, Y., Esser, P. et al. (2012). Integrin alpha3 mutations with kidney, lung, and skin disease. *N. Engl. J. Med.* **366**, 1508-1514.

Hogan, B. L. M. (1999). Morphogenesis. *Cell* **96**, 225-233.

Huang, Z., Wang, Y., Nayak, P. S., Dammann, C. E. and Sanchez-Esteban, J. (2012). Stretch-induced fetal type II cell differentiation is mediated via ErbB1-ErbB4 interactions. *J. Biol. Chem.* **287**, 18091-18102.

Isakson, B. E., Lubman, R. L., Seedorf, G. J. and Boitano, S. (2001). Modulation of pulmonary alveolar type II cell phenotype and communication by extracellular matrix and KGF. *Am. J. Physiol. Cell Physiol.* **281**, C1291-C1299.

Jones, R. G., Li, X., Gray, P. D., Kuang, J., Clayton, F., Samowitz, W. S., Madison, B. B., Gumucio, D. L. and Kuwada, S. K. (2006). Conditional deletion of beta1 integrins in the intestinal epithelium causes a loss of Hedgehog expression, intestinal hyperplasia, and early postnatal lethality. *J. Cell Biol.* **175**, 505-514.

Kauffman, S. L. (1977). Acceleration of canalicular development in lungs of fetal mice exposed transplacentally to dexamethasone. *Lab. Invest.* **36**, 395-401.

Kim, K. K., Wei, Y., Szekeres, C., Kugler, M. C., Wolters, P. J., Hill, M. L., Frank, J. A., Brumwell, A. N., Wheeler, S. E., Kreidberg, J. A. et al. (2009). Epithelial cell alpha3beta1 integrin links beta-catenin and Smad signaling to promote myofibroblast formation and pulmonary fibrosis. *J. Clin. Invest.* **119**, 213-224.

Kreidberg, J. A., Donovan, M. J., Goldstein, S. L., Rennke, H., Shepherd, K., Jones, R. C. and Jaenisch, R. (1996). Alpha 3 beta 1 integrin has a crucial role in kidney and lung organogenesis. *Development* **122**, 3537-3547.

Lakshminarayanan, V., Lewallen, M., Frangogiannis, N. G., Evans, A. J., Wedin, K. E., Michael, L. H. and Entman, M. L. (2001). Reactive oxygen intermediates induce monocyte chemotactic protein-1 in vascular endothelium after brief ischemia. *Am. J. Pathol.* **159**, 1301-1311.

Li, N., Zhang, Y., Naylor, M. J., Schatzmann, F., Maurer, F., Wintermantel, T., Schuetz, G., Mueller, U., Streuli, C. H. and Hynes, N. E. (2005). Beta1 integrins regulate mammary gland proliferation and maintain the integrity of mammary alveoli. *EMBO J.* **24**, 1942-1953.

Lwebuga-Mukasa, J. S. (1991). Matrix-driven pneumocyte differentiation. *Am. Rev. Respir. Dis.* **144**, 452-457.

Mathew, S., Lu, Z., Palamuttam, R. J., Mernaugh, G., Hadziselimovic, A., Chen, J., Bulus, N., Gewin, L. S., Voehler, M., Meves, A. et al. (2012). beta1 Integrin NPxY motifs regulate kidney collecting duct development and maintenanceby induced-fit interactions with cytosolic proteins. *Mol. Cell. Biol.* **32**, 4080-4091.

McGowan, S. E. (1992). Extracellular matrix and the regulation of lung development and repair. *FASEB J.* **6**, 2895-2904.

McKee, K. K., Capizzi, S. and Yurchenco, P. D. (2009). Scaffold-forming and adhesive contributions of synthetic laminin-binding proteins to basement membrane assembly. *J. Biol. Chem.* **284**, 8984-8994.

Menko, A. S., Kreidberg, J. A., Ryan, T. T., Van Bockstaele, E. and Kukuruzinska, M. A. (2001). Loss of alpha3beta1 integrin function results in an altered differentiation program in the mouse submandibular gland. *Dev. Dyn.* **220**, 337-349.

Miettinen, P. J., Berger, J. E., Meneses, J., Phung, Y., Pedersen, R. A., Werb, Z. and Derynck, R. (1995). Epithelial immaturity and multiorgan failure in mice lacking epidermal growth factor receptor. *Nature* **376**, 337-341.

Min, H., Danilenko, D. M., Scully, S. A., Bolon, B., Ring, B. D., Tarpley, J. E., DeRose, M. and Simonet, W. S. (1998). Fgf-10 is required for both limb and lung development and exhibits striking functional similarity to Drosophila branchless. *Genes Dev.* **12**, 3156-3161.

Morrisey, E. E. and Hogan, B. L. M. (2010). Preparing for the first breath: genetic and cellular mechanisms in lung development. *Dev. Cell* **18**, 8-23.

Naylor, M. J., Li, N., Cheung, J., Lowe, E. T., Lambert, E., Marlow, R., Wang, P., Schatzmann, F., Wintermantel, T., Schüetz, G. et al. (2005). Ablation of beta1 integrin in mammary epithelium reveals a key role for integrin in glandular morphogenesis and differentiation. *J. Cell Biol.* **171**, 717-728.

Nguyen, N. M. and Senior, R. M. (2006). Laminin isoforms and lung development: all isoforms are not equal. *Dev. Biol.* **294**, 271-279.

Nguyen, N. M., Miner, J. H., Pierce, R. A. and Senior, R. M. (2002). Laminin alpha 5 is required for lobar septation and visceral pleural basement membrane formation in the developing mouse lung. *Dev. Biol.* **246**, 231-244.

Nguyen, N. M., Kelley, D. G., Schlueter, J. A., Meyer, M. J., Senior, R. M. and Miner, J. H. (2005). Epithelial laminin alpha5 is necessary for distal epithelial cell maturation, VEGF production, and alveolization in the developing murine lung. *Dev. Biol.* **282**, 111-125.

Nicola, T., Hagood, J. S., James, M. L., MacEwen, M. W., Williams, T. A., Hewitt, M. M., Schwiebert, L., Bulger, A., Oparil, S., Chen, Y.-F. et al. (2009). Loss of Thy-1 inhibits alveolar development in the newborn mouse lung. *Am. J. Physiol. Lung Cell. Mol. Physiol.* **296**, L738-L750.

Nicolaou, N., Margadant, C., Kevelam, S. H., Lilien, M. R., Oosterveld, M. J. S., Kreft, M., van Eerde, A. M., Pfundt, R., Terhal, P. A., van der Zwaag, B. et al. (2012). Gain of glycosylation in integrin alpha3 causes lung disease and nephrotic syndrome. *J. Clin. Invest.* **122**, 4375-4387.

Nold, M. F., Mangan, N. E., Rudloff, I., Cho, S. X., Shariatian, N., Samarasinghe, T. D., Skuza, E. M., Pedersen, J., Veldman, A., Berger, P. J. et al. (2013). Interleukin-1 receptor antagonist prevents murine bronchopulmonary dysplasia induced by perinatal inflammation and hyperoxia. *Proc. Natl. Acad. Sci. USA* **110**, 14384-14389.

Okubo, T., Knoepfler, P. S., Eisenman, R. N. and Hogan, B. L. M. (2005). Nmyc plays an essential role during lung development as a dosage-sensitive regulator of progenitor cell proliferation and differentiation. *Development* **132**, 1363-1374.

Olsen, C. O., Isakson, B. E., Seedorf, G. J., Lubman, R. L. and Boitano, S. (2005). Extracellular matrix-driven alveolar epithelial cell differentiation in vitro. *Exp. Lung Res.* **31**, 461-482.

Perl, A.-K. T., Wert, S. E., Nagy, A., Lobe, C. G. and Whitsett, J. A. (2002). Early restriction of peripheral and proximal cell lineages during formation of the lung. *Proc. Natl. Acad. Sci. USA* **99**, 10482-10487.

Pozzi, A. and Zent, R. (2011). Extracellular matrix receptors in branched organs. *Curr. Opin. Cell Biol.* **23**, 547-553.

Prince, L. S., Okoh, V. O., Moninger, T. O. and Matalon, S. (2004). Lipopolysaccharide increases alveolar type II cell number in fetal mouse lungs through Toll-like receptor 4 and NF-kappaB. *Am. J. Physiol. Lung Cell. Mol. Physiol.* **287**, L999-L1006.

Prince, L. S., Dieperink, H. I., Okoh, V. O., Fierro-Perez, G. A. and Lallone, R. L. (2005). Toll-like receptor signaling inhibits structural development of the distal fetal mouse lung. *Dev. Dyn.* **233**, 553-561.

Raghavan, S., Bauer, C., Mundschau, G., Li, Q. and Fuchs, E. (2000). Conditional ablation of beta1 integrin in skin: severe defects in epidermal proliferation, basement membrane formation, and hair follicle invagination. *J. Cell Biol.* **150**, 1149-1160.

Rannels, D. E. and Rannels, S. R. (1989). Influence of the extracellular matrix on type 2 cell differentiation. *Chest* **96**, 165-173.

Rice, W. R., Conkright, J. J., Na, C. L., Ikegami, M., Shannon, J. M. and Weaver, T. E. (2002). Maintenance of the mouse type II cell phenotype in vitro. *Am. J. Physiol. Lung Cell. Mol. Physiol.* **283**, L256-L264.

Sanchez-Esteban, J., Wang, Y., Gruppuso, P. A. and Rubin, L. P. (2004). Mechanical stretch induces fetal type II cell differentiation via an epidermal growth factor receptor-extracellular-regulated protein kinase signaling pathway. *Am. J. Respir. Cell Mol. Biol.* **30**, 76-83.

Sekine, K., Ohuchi, H., Fujiwara, M., Yamasaki, M., Yoshizawa, T., Sato, T., Yagishita, N., Matsui, D., Koga, Y., Itoh, N. et al. (1999). Fgf10 is essential for limb and lung formation. *Nat. Genet.* **21**, 138-141.

Taddei, I., Deugnier, M.-A., Faraldo, M. M., Petit, V., Bouvard, D., Medina, D., Fässler, R., Thiery, J. P. and Glukhova, M. A. (2008). Beta1 integrin deletion from the basal compartment of the mammary epithelium affects stem cells. *Nat. Cell Biol.* **10**, 716-722.

Tanjore, H., Degryse, A. L., Crossno, P. F., Xu, X. C., McConaha, M. E., Jones, B. R., Polosukhin, V. V., Bryant, A. J., Cheng, D.-S., Newcomb, D. C. et al. (2013). beta-catenin in the alveolar epithelium protects from lung fibrosis after intratracheal bleomycin. *Am. J. Respir. Crit. Care Med.* **187**, 630-639.

Thibeault, D. W., Mabry, S. M., Ekekezie, I. I., Zhang, X. and Truog, W. E. (2003). Collagen scaffolding during development and its deformation with chronic lung disease. *Pediatrics* **111**, 766-776.

Urich, D., Eisenberg, J. L., Hamill, K. J., Takawira, D., Chiarella, S. E., Soberanes, S., Gonzalez, A., Koentgen, F., Manghi, T., Hopkinson, S. B. et al. (2011). Lung-specific loss of the laminin alpha3 subunit confers resistance to mechanical injury. *J. Cell Sci.* **124**, 2927-2937.

Vlahos, R., Stambas, J., Bozinovski, S., Broughton, B. R. S., Drummond, G. R. and Selemidis, S. (2011). Inhibition of Nox2 oxidase activity ameliorates influenza A virus-induced lung inflammation. *PLoS Pathog.* **7**, e1001271.

Wang, Y., Maciejewski, B. S., Lee, N., Silbert, O., McKnight, N. L., Frangos, J. A. and Sanchez-Esteban, J. (2006). Strain-induced fetal type II epithelial cell differentiation is mediated via cAMP-PKA-dependent signaling pathway. *Am. J. Physiol. Lung Cell. Mol. Physiol.* **291**, L820-L827.

Wang, Y., Maciejewski, B. S., Soto-Reyes, D., Lee, H.-S., Warburton, D. and Sanchez-Esteban, J. (2009). Mechanical stretch promotes fetal type II epithelial cell differentiation via shedding of HB-EGF and TGF-alpha. *J. Physiol.* **587**, 1739-1753.

Development (2014) 141, 4751-4762 doi:10.1242/dev.117200

Wang, Y., Huang, Z., Nayak, P. S., Matthews, B. D., Warburton, D., Shi, W. and Sanchez-Esteban, J. (2013). Strain-induced differentiation of fetal type II epithelial cells is mediated via the integrin alpha6beta1-ADAM17/tumor necrosis factor-alpha-converting enzyme (TACE) signaling pathway. *J. Biol. Chem.* **288**, 25646-25657.

Wasowicz, M., Biczysko, W., Marszalek, A., Yokoyama, S. and Nakayama, I. (1998). Ultrastructural studies on selected elements of the extracellular matrix in the developing rat lung alveolus. *Folia Histochem. Cytobiol.* **36**, 3-13.

Weinstein, M., Xu, X., Ohyama, K. and Deng, C. X. (1998). FGFR-3 and FGFR-4 function cooperatively to direct alveogenesis in the murine lung. *Development* **125**, 3615-3623.

Willem, M., Miosge, N., Halfter, W., Smyth, N., Jannetti, I., Burghart, E., Timpl, R. and Mayer, U. (2002). Specific ablation of the nidogen-binding site in the laminin gamma1 chain interferes with kidney and lung development. *Development* **129**, 2711-2722.

Xing, L. and Remick, D. G. (2007a). Mechanisms of oxidant regulation of monocyte chemotactic protein 1 production in human whole blood and isolated mononuclear cells. *Shock* **28**, 178-185.

Xing, L. and Remick, D. G. (2007b). Promoter elements responsible for antioxidant regulation of MCP-1 gene expression. *Antioxid. Redox Signal.* **9**, 1979-1990.

Yamashita, S., Maeshima, A., Kojima, I. and Nojima, Y. (2004). Activin A is a potent activator of renal interstitial fibroblasts. *J. Am. Soc. Nephrol.* **15**, 91-101.

Young, L. R., Gulleman, P. M., Bridges, J. P., Weaver, T. E., Deutsch, G. H., Blackwell, T. S. and McCormack, F. X. (2012). The alveolar epithelium determines susceptibility to lung fibrosis in Hermansky-Pudlak syndrome. *Am. J. Respir. Crit. Care Med.* **186**, 1014-1024.

Zaynagetdinov, R., Sherrill, T. P., Polosukhin, V. V., Han, W., Ausborn, J. A., McLoed, A. G., McMahon, F. B., Gleaves, L. A., Degryse, A. L., Stathopoulos, G. T. et al. (2011). A critical role for macrophages in promotion of urethane-induced lung carcinogenesis. *J. Immunol.* **187**, 5703-5711.

Zhang, X., Mernaugh, G., Yang, D.-H., Gewin, L., Srichai, M. B., Harris, R. C., Iturregui, J. M., Nelson, R. D., Kohan, D. E., Abrahamson, D. et al. (2009). beta1 integrin is necessary for ureteric bud branching morphogenesis and maintenance of collecting duct structural integrity. *Development* **136**, 3357-3366.

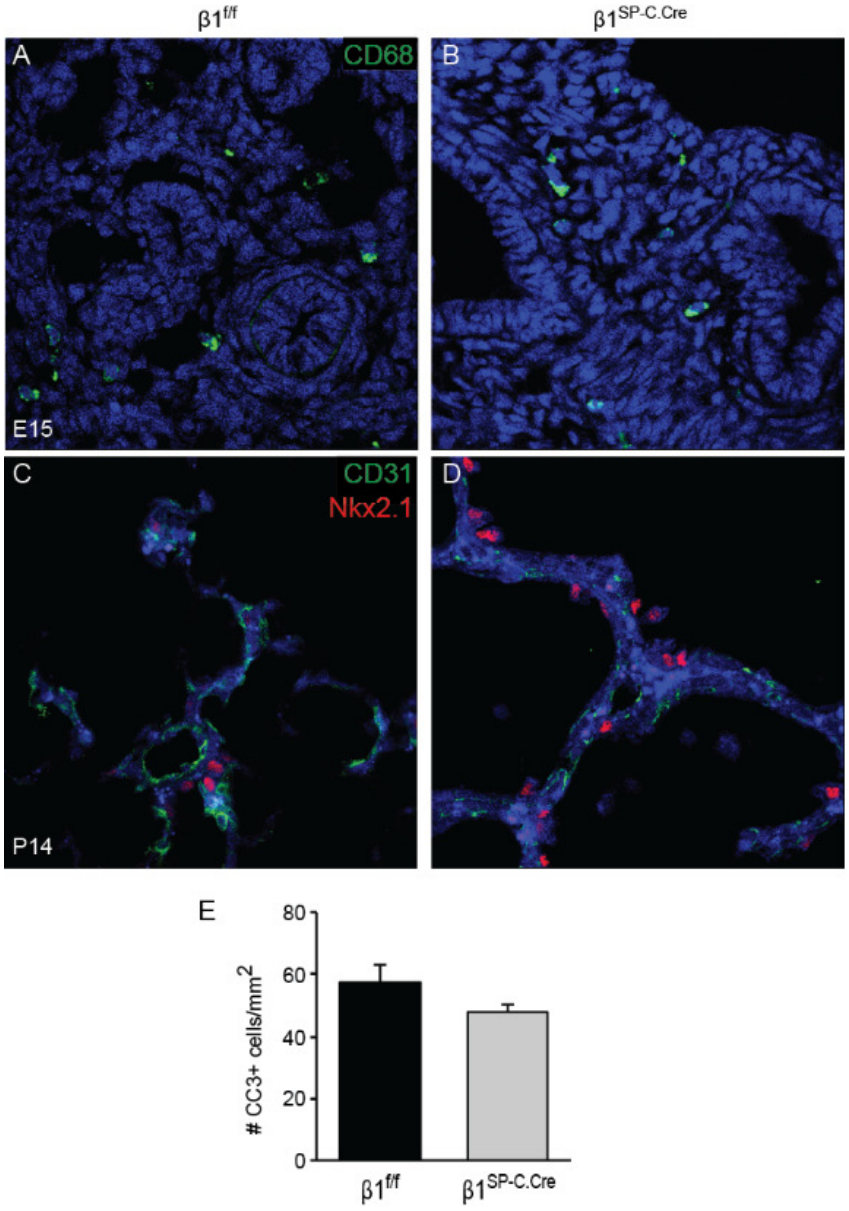

Supplemental Figure 1

Supplemental Figure 1. Epithelial β1 integrin deletion results in increased macrophage accumulation after E15 and retains an intact capillary network at P14. (A, B) E15 frozen sections immunostained for CD68 (green) show similar numbers of macrophages present in control (A) and $\beta1^{SP\text{-}C.Cre}$ (B) lungs. (C, D) P14 frozen sections immunostained for the vascular marker CD31 (green) and Nkx2.1 (red) demonstrate an intact capillary network in close proximity to the alveolar surface in both control (C) and $\beta1^{SP\text{-}C.Cre}$ (D) lungs. (E) The number of cleaved caspase-3 (CC3) + cells/mm^2 is not significantly different between E18 $\beta1^{SP\text{-}C\ Cre}$ and $\beta1^{f/f}$ lungs.